Chem Biol Drug Des 2010; **75:** 481–488

Research Article

doi: 10.1111/j.1747-0285.2010.00961.x

Inhibition of Tubulogenesis and of Carcinogen-mediated Signaling in Brain Endothelial Cells Highlight the Antiangiogenic Properties of a Mumbaistatin Analog

Elizabeth Tahanian[1], Simon Lord-Dufour[1], Abhirup Das[2], Chaitan Khosla[2], René Roy[3] and Borhane Annabi[1,3]*

[1]*Centre de Recherche BioMED, Université du Québec à Montréal, QC, Canada H3C 3P8*

[2]*Departments of Chemistry, Chemical Engineering and Biochemistry, Stanford University, Stanford, CA, USA*

[3]*Centre de Recherche PharmaQAM, Université du Québec à Montréal, QC, Canada, H3C 3P8*

**Corresponding author: Borhane Annabi, annabi.borhane@uqam.ca*

A better understanding of the metabolic adaptations of the vascular endothelial cells (EC) that mediate tumor vascularization would help the development of new drugs and therapies. Novel roles in cell survival and metabolic adaptation to hypoxia have been ascribed to the microsomal glucose-6-phosphate translocase (G6PT). While antitumorigenic properties of G6PT inhibitors such as chlorogenic acid (CHL) have been documented, those of the G6PT inhibitor and semi-synthetic analog AD4-015 of the polyketide mumbaistatin are not understood. In the present study, we evaluated the *in vitro* antiangiogenic impact of AD4-015 on human brain microvascular endothelial cells (HBMEC), which play an essential role as structural and functional components in tumor angiogenesis. We found that *in vitro* HBMEC migration and tubulogenesis were reduced by AD4-015 but not by CHL. The mumbaistatin analog significantly inhibited the phorbol 12-myristate 13-acetate (PMA)-induced matrix-metalloproteinase (MMP)-9 secretion and gene expression as assessed by zymography and RT-PCR. PMA-mediated cell signaling leading to cyclooxygenase (COX)-2 expression and IκB downregulation was also inhibited, further confirming AD4-015 as a cell signaling inhibitor in tumor promoting conditions. G6PT functions may therefore account for the metabolic flexibility that enables EC-mediated neovascularization. This process could be specifically targeted within the vasculature of developing brain tumors by G6PT inhibitors.

Key words: angiogenesis, brain endothelial cells, carcinogenesis, COX-2, G6PT inhibitors, MMP-9

Abbreviations: BBB, blood–brain barrier; COX-2, cyclooxygenase-2; EC, endothelial cells; G6PT, glucose-6-phosphate translocase; HBMEC, human brain microvascular EC; MMP-9, matrix metalloproteinase-9; PMA, phorbol 12-myristate 13-acetate.

Received 21 December 2009, revised 03 February 2010 and accepted for publication 06 February 2010

Tumor-associated angiogenesis, a fundamental process in cancer tissue growth, consists of recruiting endothelial cells (EC) toward an angiogenic stimulus (1). The cells subsequently proliferate and differentiate to form endothelial tubes and capillary-like structures. Although little is known about the metabolic adaptation of EC through such a transformation, it has been suggested that the inhibition of metabolic pathways may offer a novel and powerful therapeutic approach that would simultaneously inhibit tumor cell proliferation and tumor-induced angiogenesis (2,3). In fact, brain tumor–associated microvasculature is thought to become aberrant and to undergo a sequence of adaptive changes, such as during the development of gliomas. These changes are characterized by important metabolic adaptations, primarily involving hypoxia-regulated genes (4). Among those, transcription of genes responsible for glucose and energy metabolism, such as glucose transporters and glycolytic enzymes, has been documented. These proteins take up glucose and convert it to lactate, and include pyruvate dehydrogenase kinase 1, which shunts pyruvate away from the mitochondria, and BNIP3, which triggers selective mitochondrial autophagy (5). The adaptative shift from oxidative to glycolytic metabolism also allows maintenance of redox homeostasis and cell survival under conditions of prolonged hypoxia.

Recently, our group ascribed a dual role to the microsomal glucose-6-phosphate translocase (G6PT) in cell survival and metabolic adaptation to hypoxia in cancer cells and in hypoxic cells (6–8). In fact, hypoxia inducible factor (HIF)-1α was found to regulate G6PT gene expression (8). G6PT has originally been shown to transport G6P from the cytosol to the lumen of the endoplasmic reticulum, thereby performing the rate-limiting step for G6P hydrolysis into glucose and inorganic phosphate by the glucose-6-phosphatase system (9). G6PT is also known to integrate and regulate many metabolic functions such as glycemia, lipidemia, uricemia, and lactic acidemia (10). More importantly, its activity cannot be substituted as G6PT deficiencies lead to glycogen storage disease type Ib characterized

not only by disturbed glucose homeostasis but also by severe myeloid dysfunctions (10). G6PT was further shown to play a role in bone marrow cell and neutrophil chemotaxis (11,12), in calcium flux control (13–16), and in U87 glioma cell survival (6,7). In turn, G6PT gene expression is regulated in response to adaptive metabolic changes involving glucose, insulin and cyclic AMP (17). G6PT-mediated metabolic adaptation, which could enable cells to survive under conditions characterized by hypoxia (8) may therefore become an appealing therapeutic prospect through the design of efficient anti-G6PT molecules targeting those cells proliferating within the tumor microenvironment.

Among anti-G6PT targeting strategies, the anthraquinone natural product mumbaistatin is one of the most potent known functional inhibitors of G6PT. Its availability, however, has been limited because of its extremely low yields from the natural source cultures of *Streptomyces* sp. (18). A facile semisynthetic method that afforded high yields and generation of a variety of mumbaistatin analogs within five steps was therefore developed starting from DMAC (5,3,8-dihydroxyanthraquinone-2-carboxylic acid), a structurally related polyketide product of engineered biosynthesis (19). Among those semisynthetic analog of the polyketide mumbaistatin, AD4-015 was found by us to potently and specifically reduce cell survival of those cells that adapted to hypoxia (8). Such anti-G6PT effect was better than that of chlorogenic acid (CHL), whose pharmacological functions also target G6P transport functions (20) and, in recent years, shown to affect hepatoma and glioblastoma cell proliferation and survival (21,22). Collectively, our data therefore suggest that G6PT may account for important molecular adaptation that enables cells to survive under conditions characterized by hypoxia and could be specifically targeted within developing tumors. To date, no roles for G6PT have yet been proposed in angiogenesis, and little is known about metabolic targeting of tumor-associated EC as part of cancer treatments.

Human brain microvascular endothelial cells (HBMEC) play an essential role as structural and functional components of the blood–brain barrier (BBB). Most importantly, recent studies delineated a unique adaptative phenotype of brain EC in which matrix metalloproteinase (MMP)-9 secretion in HBMEC was increased by the tumor-promoting agent phorbol 12-myristate 13-acetate (23,24), a condition that favors disruption of the BBB by MMP-9 and tumor invasion (25). Given that HBMEC play a role in angiogenesis within hypoxic tumors, we questioned in this study whether the semi-synthetic analog of the polyketide mumbaistatin, a potent G6PT inhibitor, could target HBMEC's angiogenic properties including carcinogen-induced MMP-9 secretion, cell migration and *in vitro* tubulogenesis.

Materials and Methods

Materials

Sodium dodecylsulfate (SDS) and bovine serum albumin (BSA) were purchased from Sigma (Oakville, ON, USA). Electrophoresis reagents were purchased from Bio-Rad (Mississauga, ON, USA). The enhanced chemiluminescence (ECL) reagents were from Perkin Elmer (Waltham, MA, USA). Micro bicinchoninic acid protein assay reagents were from Pierce (Rockford, IL, USA). All other reagents were from Sigma–Aldrich Canada.

Cell culture

Human brain microvascular endothelial cells were characterized and generously provided by Dr Kwang Sik Kim of Johns Hopkins University School of Medicine (Baltimore, MD, USA). These cells were positive for factor VIII-Rag, carbonic anhydrase IV and Ulex Europeus Agglutinin I; they took up fluorescently labeled, acetylated low-density lipoprotein and expressed gamma glutamyl transpeptidase, demonstrating their brain EC-specific phenotype (26). Human brain microvascular endothelial cells were immortalized by transfection with simian virus 40 large T antigen and maintained their morphological and functional characteristics for at least 30 passages (27). Human brain microvascular endothelial cells were maintained in RPMI 1640 (Gibco, Burlington, ON, USA) supplemented with 10% (v/v) heat-inactivated fetal bovine serum (HyClone Laboratories, Logan, UT, USA), 10% (v/v) NuSerum (BD Bioscience, Mountain View, CA, USA), modified Eagle's medium non-essential amino acids (1%) and vitamins (1%) (Gibco), sodium pyruvate (1 mM) and EC growth supplement (30 μg/mL). Cells were cultured at 37 °C under a humidified atmosphere containing 5% CO_2. All experiments were performed using passages 3–28.

cDNA synthesis and semi-quantitative real-time RT-PCR

Total RNA was extracted from cultured HBMEC using TRIzol reagent (Invitrogen, Burlington, ON, USA). Semi-quantitative RT-PCR analysis was performed starting with 2 μg of total RNA for first strand cDNA synthesis, followed by specific gene product amplification with the One-Step RT-PCR kit (Invitrogen). Primers for MMP-9 (forward: 5′-AAGATGCTGCTGTTCAGCGGG-3′, reverse: 5′-GTCCTCAG GGCACTGCAGGAT-3′) were derived from human sequences. PCR conditions were optimized so that the gene products were examined at the exponential phase of their amplification, and the products were resolved on 1.8% agarose gels containing 1 μg/mL ethidium bromide.

Analysis of HBMEC migration

Human brain microvascular endothelial cells migration was assessed using modified Boyden chambers. The lower surfaces of Transwells (8-μm pore size; Costar, Acton, MA, USA) were precoated with 0.2% type-I collagen for 2 h at 37 °C. The Transwells were then assembled in a 24-well plate (Fisher Scientific Ltd, Nepean, ON, USA). The lower chamber was filled with serum-free HBMEC medium in the presence or absence of the G6PT inhibitors. Human brain microvascular endothelial cells were collected by trypsinization, washed and resuspended in serum-free medium at a concentration of 10^6 cells/mL; 10^5 cells were then inoculated onto the upper side of each modified Boyden chamber. The plates were placed at 37 °C in 5% CO_2/95% air for 30 min after which various concentrations of G6PT inhibitors were added to the lower chambers of the Transwells. Migration then proceeded for 6 h at 37 °C in 5% CO_2/95% air. Cells that had migrated to the lower surfaces of the filters were fixed with 3.7% formaldehyde and stained with

0.1% crystal violet-20% methanol (v/v). Images of at least five random fields per filter were digitized (10× magnification). The average number of migrating cells per field was quantified using Northern Eclipse software (Empix Imaging Inc., Mississauga, ON, USA). Migration data are expressed as a mean value derived from at least three independent experiments.

Endothelial cell morphogenesis assay

Tubulogenesis was assessed using Matrigel aliquots of 50 μL, plated into individual wells of 96-well tissue culture plates (Costar, Amherst, MA, USA) and allowed to polymerize at 37 °C for 30 min. After brief trypsinization, HBMEC were washed and resuspended at a concentration of 2.5×10^5 cells/mL in serum-free medium. One hundred microlitre of cell suspension (25 000 cells/well) and 75 μL of medium with serum were added into each culture well. Cells were allowed to form capillary-like tubes at 37 °C in 5% CO_2/95% air for 18 h in the presence or absence of different AD4-015 concentrations. The formation of capillary-like structures was examined microscopically, and pictures (10×) were taken using a Retiga 1300 camera (QImaging, Surrey, BC, Canada) and a Nikon Eclipse TE2000-U microscope. The extent to which capillary-like structures formed in the gel was quantified by analysis of digitized images to determine the thread length of the capillary-like network, using a commercially available image analysis program (Northern Eclipse) as described and validated previously (28,29). For each experiment, four randomly chosen areas were quantified by counting the number of tubes formed. Tubulogenesis data are expressed as a mean value derived from at least three independent experiments.

Gelatin zymography

Gelatin zymography was used to assess the extent of proMMP-2 and proMMP-9 activity as previously described (30). Briefly, an aliquot (20 μL) of the culture medium was subjected to SDS-PAGE in a gel containing 0.1 mg/mL gelatin. The gels were then incubated in 2.5% Triton X-100 and rinsed in nanopure distilled H_2O. Gels were further incubated at 37 °C for 20 h in 20 mM NaCl, 5 mM $CaCl_2$, 0.02% Brij-35, 50 mM Tris–HCl buffer, pH 7.6, then stained with 0.1% Coomassie Brilliant blue R-250 and destained in 10% acetic acid, 30% methanol in H_2O. Gelatinolytic activity was detected as unstained bands on a blue background.

Immunoblotting procedures

Cytosolic proteins from control and treated cells were separated by SDS–polyacrylamide gel electrophoresis (PAGE). After electrophoresis, proteins were electrotransferred onto polyvinylidene difluoride membranes, which were then blocked for 1 h at room temperature with 5% non-fat dry milk in Tris-buffered saline (150 mM NaCl, 20 mM Tris–HCl, pH 7.5) containing 0.1% Tween-20 (TBST). Membranes were further washed in TBST and incubated with the primary polyclonal anti-HuR antibody (1/1000 dilution; Jackson ImmunoResearch Laboratories, West Grove, PA, USA) in TBST containing 3% BSA, followed by a 1-h incubation with horseradish peroxidase–conjugated anti-rabbit IgG (1/2500 dilution) in TBST containing 5% non-fat dry milk. Immunoreactive material was visualized by ECL.

Cell survival assay

Cell survival was assessed by measuring fluorometric caspase-3 activity. Human brain microvascular endothelial cells were grown to 60% confluence and treated with different concentrations of the mumbaistatin analog. Cells were collected and washed in ice-cold PBS pH 7.0. Cells were subsequently lysed in Apo-Alert lysis buffer (Clontech, Palo Alto, CA, USA) for one hour at 4 °C, and the lysates were clarified by centrifugation at 16 000 × g for 20 min. Caspase-3 activity was determined by incubation with 50 μM of the caspase-3-specific fluorogenic peptide substrate acetyl-Asp-Glu-Val-Asp-7-amino-4-trifluoromethylcoumarin (Ac-DEVD-AFC) in assay buffer [50 mM Hepes-NaOH (pH 7.4), 100 mM NaCl, 10% sucrose, 0,1% 3-[(3-cholamidopropyl) dimethylammonio]-1-propanesulfonate, 5 mM DTT and 1 mM EDTA] in 96-well plates (31). The release of AFC was monitored for at least 30 min at 37 °C on a fluorescence plate reader (Molecular Dynamics) (λ_{ex} = 400 nm, λ_{em} = 505 nm).

Statistical data analysis

Data are representative of three or more independent experiments. Statistical significance was assessed using Student's unpaired t-test and probability values of <0.05 were considered significant; an asterisk (*) identifies such significance in each figure.

Results

Polyketide derivative AD4-015 inhibits in vitro HBMEC cell migration

The effects of CHL (Figure 1A upper panel), a natural product with weak G6PT inhibitory activity (20) and of a more potent semi-synthetic polyketide analog (AD4-015, Figure 1A middle panel) of a different natural product, mumbaistatin (19) (Figure 1A lower panel), were tested on HBMEC migration (Figure 1B). While CHL had no significant effect, HBMEC migration was inhibited dose-dependently by AD4-015 with a calculated IC_{50} of 11.2 ± 3.1 μM (Figure 1C). Because AD4-015 must cross the plasma membrane, this level of inhibition by AD4-015 is slightly higher than those IC_{50} parameters ascertained from dose–response curves generated for G6PT inhibition in acellular rat liver microsomal assays (IC_{50} of 2.5 μM) (19). The latter assay allowing direct inhibition of [^{14}C]G6P transport/hydrolysis functions performed by the microsomal glucose-6-phosphatase system (9).

Mumbaistatin analog AD4-015 inhibits HBMEC in vitro *capillary-like structure formation*

In order to next assess the antiangiogenic potential of G6PT inhibitors, we used the classical Matrigel angiogenesis assay (32). Cells were seeded on top of Matrigel and left to adhere as described in the Methods section. Various concentrations of AD4-015 were then added, and capillary formation was left to proceed for 18 h. While a well-defined capillary-like network formed in vehicle-treated cells (Figure 2A), tubulogenesis was inhibited by AD4-015 with an IC_{50} of 3.5 ± 0.8 μM (Figure 2B, closed circles). Cell viability, based on caspase-3 activity, was not significantly affected by AD4-015 (Figure 2B, open circles). Lack of cytotoxic effect, combined with the inhibition of structure formation within Matrigel, prompted us to

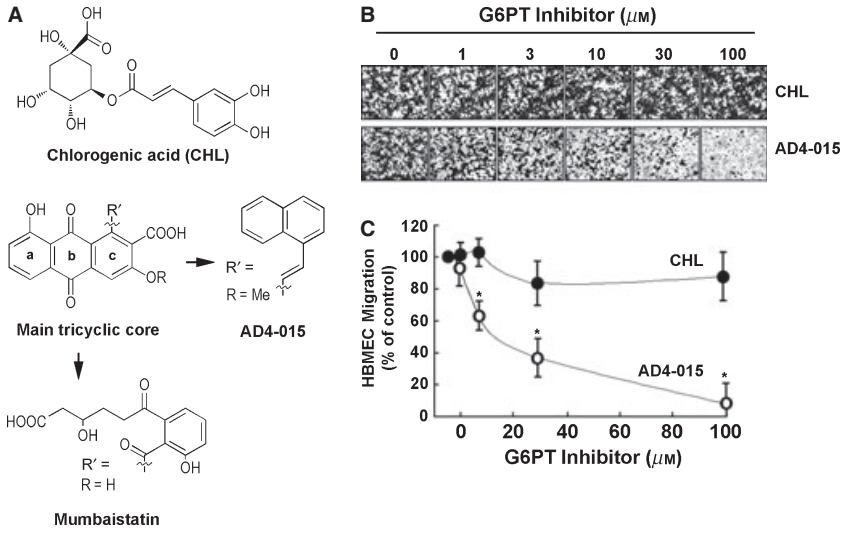

Figure 1: Polyketide derivative AD4-015 inhibits *in vitro* human brain microvascular endothelial cells (HBMEC) cell migration. (A) Structures of chlorogenic acid (CHL), parental mumbaistatin and AD4-015. Mumbastatin and AD4-015 have the same main tricyclic core; the hydroxyl group of ring c present in mumbaistatin has been exchanged by a methoxy group, and the ketone moiety by a trans-alkene naphthalenyl group to generate AD4-015. (B) HBMEC were treated with varying CHL or AD4-015 concentrations. At the end of the treatment, cells were harvested and seeded on top of gelatin-coated filters using modified Boyden chambers. Migration proceeded for 6 h, and pictures were taken of the stained filters. (C) Densitometric quantification of cell migration was performed from stained filters of AD4-015- (open circles) and CHL- (closed circles)-treated HBMEC.

investigate whether any extracellular matrix (ECM) degrading events were involved in AD4-015 inhibition.

AD4-015 inhibits PMA-induced MMP-9 gene expression and secretion in HBMEC

Among the secreted enzymes involved in ECM degradation, MMP are well documented as being involved in cell migration and tubulogenesis (23,33). More specifically, MMP-2 and MMP-9 are secreted by numerous cell types and their presence is often representative of angiogenesis (34,35). Human brain microvascular endothelial cells were serum-starved, treated for 18 h with AD4-015, and the conditioned medium was harvested. The levels of MMP-2 and of MMP-9 were measured by gelatin zymography in media samples derived from control and phorbol 12-myristate 13-acetate (PMA)-treated cells. While extracellular MMP-2 levels remained unaffected by PMA or AD4-015, MMP-9 activity was significantly increased upon PMA treatment (Figure 3A). Addition of AD4-015 to PMA-treated cells resulted in inhibition of extracellular MMP-9 activity (Figure 3A). Consistent with this observation, PMA increased MMP-9 gene expression in HBMEC, whereas AD4-015 blocked this increase in a dose-dependent fashion (Figure 3B).

AD4-015 antagonizes carcinogen-mediated cell signaling leading to COX-2 expression in HBMEC

Cyclooxygenase (COX)-2 expression is increased in tumor-associated inflammation and angiogenesis (36). Recently, the antiangiogenic effect of statins was explained by their ability to inhibit COX-2 and MMP-9 in human EC (37). In order to better understand the effect

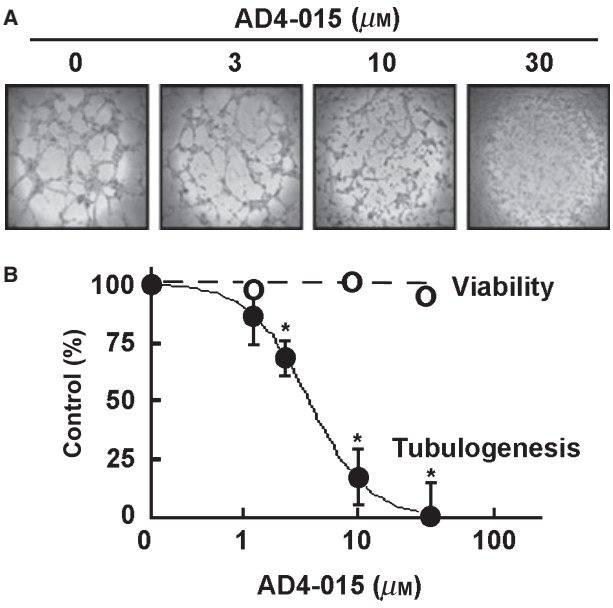

Figure 2: Polyketide derivative AD4-015 inhibits human brain microvascular endothelial cells (HBMEC) *in vitro* capillary-like structure formation. (A) In order to assess *in vitro* tubulogenesis, HBMEC were seeded on top of Matrigel as described in the Methods section, and then treated with varying concentrations of AD4-015 for 18 h. Representative phase contrast pictures are shown. (B) The extent of cell survival (open circles) and of three-dimensional capillary-like structure formation (closed circles) was quantified as described in the Methods section. Data are presented as percent of vehicle-treated cells (control).

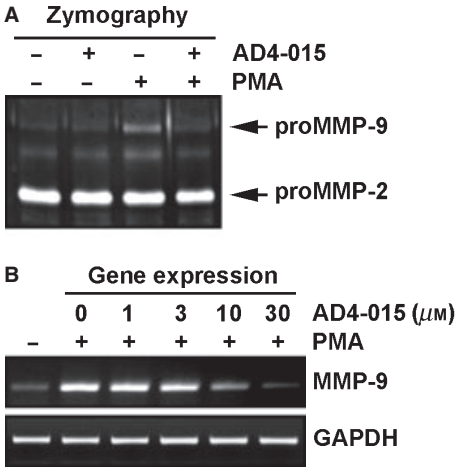

Figure 3: AD4-015 inhibits phorbol 12-myristate 13-acetate (PMA)-induced matrix metalloproteinase (MMP)-9 gene expression and secretion in human brain microvascular endothelial cells (HBMEC). HBMEC were serum-starved in the presence of 30 μM AD4-015, 1 μM PMA, or a combination of both for 18 h. (A) Conditioned media were then harvested and gelatin zymography was performed in order to detect proMMP-9 and proMMP-2 hydrolytic activity as described in the Methods section. (B) Total RNA was extracted from HBMEC treated with various concentrations of AD4-015 as described in the Methods section. Semi-quantitative RT-PCR was performed to confirm the presence of a single amplicon for MMP-9 and for GAPDH. Data are representative of three independent experiments.

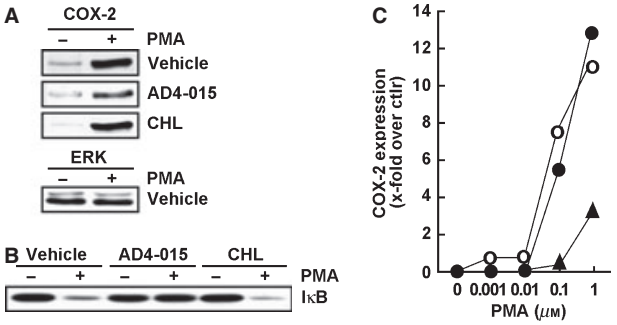

Figure 4: AD4-015 antagonizes carcinogen-mediated cell signaling leading to COX-2 expression in human brain microvascular endothelial cells (HBMEC). Lysates of serum-starved phorbol 12-myristate 13-acetate (PMA)-treated HBMEC were isolated after various co-treatments (1 μM PMA, 30 μM AD4-015, 100 μM chlorogenic acid (CHL)], electrophoresed via SDS-PAGE and immunodetection performed of (A) COX-2 and of ERK proteins, or (B) IκB performed as described in the Methods section. (C) Dose–response of PMA treatment was performed and COX-2/ERK expression was quantified by scanning densitometry of the autoradiograms (Vehicle, closed circles; CHL, open circles, AD4-015, closed triangles). Data are expressed as the x-fold induction over untreated basal conditions.

of AD4-015 on PMA-induced cell signaling in HBMEC, cells were treated with PMA in the presence of either CHL or AD4-015, and COX-2 expression was evaluated in cell lysates. PMA-induced COX-2 expression in HBMEC, and AD4-015 efficiently inhibited this increase (Figure 4A) in a dose-dependent manner (Figure 4C). In contrast, total extracellular signal–regulated kinase (ERK) expression was unaffected by CHL, which was also unable to block PMA-induced COX-2 expression (Figure 4A). The effect of AD4-015 was possibly mediated through preventing dissociation of the inhibitor of nuclear factor kappaB (IκB) from the NF-κB complex, which is rapidly degraded through an ubiquitin-mediated process (Figure 4B).

Discussion

G6P is not only an intermediate in all major metabolic pathways for glucose utilization and biosynthesis but is also an allosteric regulator of enzyme activity and gene expression. Such crucial roles for G6P have given rise to a possible subcellular compartmentation of G6P pools that may channel flux through multiple pathways (38). As such, cytoplasmic G6P levels are also strategically positioned to link the cell's energy state to the regulation of multiple functions, including for example its pro-inflammatory response to certain stresses (39). Among newly discovered intracellular glucose generating systems, a microsomal glucose-6-phosphatase complex composed of a G6PT and a G6Pase-β catalytic subunit isoform (G6PC-3) is thought to be capable of endogenous glucose production in brain (40). Whether this complex is regulated in brain EC is unknown. Interestingly, transcriptional regulation of G6PT, but not of G6PC-3, by hypoxia through HIF-1α is suggestive of metabolic adaptation to low oxygen such as that present in developing tumors (8). While the physiological consequences of this specific adaptive phenotype remain to be elucidated, alternate roles for G6PT in chemotaxis, intracellular calcium flux control, and cell survival have already been proposed. Altogether, those documented G6PT-regulated cellular functions are a common feature also found in tumor growth factors' paracrine regulation of angiogenesis (1). The novelty of our study therefore demonstrates that the G6PT inhibitor AD4-015 may act as a potent antiangiogenic agent in that it inhibits *in vitro* tubulogenesis and HBMEC migration, both of which may be modulated through G6PT metabolic control.

It is well known that angiogenesis and hypoxia determine the vessel density of a tumor, partially through the modulation of glucose transporter expression by several other genes (41). Among these, a significant correlation of HIF-1α to GLUT-1 and GLUT-3 expression was found in renal cell carcinomas (42), MCF7 breast cancer cells (43) and in hepatoma models (44). Hypoxia inducible factor-1α-induced glycolytic enzymes, including HKI, HKII, PFK-L, ALD-A, ALD-C, PGK1, ENO-alpha, PYK-M2, LDH-A and PFKFB-3, were also examined in cancer cells. It was concluded that targeting the HIF-1α-induced glucose transporter and hexokinase might provide better therapeutic targets for inhibiting tumor growth and progression than would targeting HIF-1α itself (45). Accordingly, this strategy was recently put forward in the targeting of hypoxic mesenchymal stromal cells (8), which are believed to be recruited and to contribute to brain tumor growth (46,47). It remains unknown whether metabolic targeting could be used as a therapeutic strategy.

Only recently have brain EC been considered as targets for antiangiogenic agents but also for ionizing radiation modalities in highly

vascularized tumors such as glioblastoma (28,48). Here, we have shown that the G6PT inhibitor AD4-015 inhibits MMP-9 and COX-2 expression. Recent studies have delineated a unique brain endothelial phenotype in which MMP-9 secretion in HBMEC was increased by the tumor-promoting agent PMA (23,24). MMP-9 is required for EC migration and tube formation, and inhibition of MMP-9 secretion was demonstrated to reduce both *in vitro* invasion and angiogenesis in human microvascular EC (49). Therefore, one major implication of our study is that any therapeutic strategies resulting from discovery of lead products, such as AD4-015, and which inhibit endothelial MMP-9 expression, are likely to be of utility in treating brain tumor–associated angiogenesis. Interestingly, small molecule inhibitors of MMP-9 secretion, such as the green tea polyphenol epigallocatechin gallate and the isothiocyanate sulforaphane, do so by decreasing the expression of the MMP-9 mRNA stabilizing factor HuR (23,50). Given that HuR levels are elevated in cancer (51) and have a pivotal role in promoting angiogenesis (52,53), it remains to be determined whether HuR expression is also affected upon AD4-015 treatment. The inhibition of PMA-induced MMP-9 secretion by the G6PT inhibitor AD4-015 is therefore of importance, given that MMP-9 is significantly increased during tumor progression and is associated with the opening of the BBB.

Until recently, most of the antiangiogenic or anticancerous studies performed on EC *in vitro* involved macrovascular endothelial models such as human umbilical vein EC or bovine aortic EC. However, microvascular EC, such as brain EC, display a selective phenotype that differs from macrovascular EC. The availability of a stable human model of brain EC has only very recently allowed the emergence of studies that can now more closely represent cerebral endothelial microvasculature and mimic the impact of anticancerous treatments on the brain vasculature (54). Our study is thus among the pioneering ones that are being reported. Currently, the HBMEC model is the best surrogate model that approximates tumor-derived EC available for long-term *in vitro* studies (26,28,55). Although human EC isolated from glioblastoma specimens have also been studied, these cells are not ideal targets for long-term *in vitro* studies as they de-differentiate in culture and have inherently limited proliferative potential before senescence (56).

In summary, we have provided pharmacological evidence for the role of G6PT in EC-mediated neovascularization. The activity of the semisynthetic polyketide AD4-015 in our assays represents a first step toward targeting angiogenic processes within the vasculature of developing brain tumors using small molecules.

Acknowledgments

BA and RR respectively hold a Canada Research Chair in Molecular Oncology from the Canadian Institutes of Health Research (CIHR) and a Canada Research Chair in Medicinal Chemistry from the Natural Sciences and Engineering Research Council of Canada (NSERC). This study was funded by a grant from the United States National Institutes of Health to CK (CA 77248), and by a grant of Le Fonds Québécois de la Recherche sur la Nature et les Technologies (FQRNT) to BA and RR.

References

1. Vizán P., Sánchez-Tena S., Alcarraz-Vizán G., Soler M., Messeguer R., Pujol M.D., Lee W.N., Cascante M. (2009) Characterization of the metabolic changes underlying growth factor angiogenic activation: identification of new potential therapeutic targets. Carcinogenesis;30:946–952.
2. Cascante M., Boros L.G., Comin-Anduix B., de Atauri P., Centelles J.J., Lee P.W. (2002) Metabolic control analysis in drug discovery and disease. Nat Biotechnol;20:243–249.
3. Boros L.G., Cascante M., Lee W.N. (2002) Metabolic profiling of cell growth and death in cancer: applications in drug discovery. Drug Discov Today;7:364–372.
4. Semenza G.L. (2010) Defining the role of hypoxia-inducible factor 1 in cancer biology and therapeutics. Oncogene;29:625–634.
5. Semenza G.L. (2010) HIF-1: upstream and downstream of cancer metabolism. Curr Opin Genet Dev;20:51–56.
6. Belkaid A., Copland I.B., Massillon D., Annabi B. (2006) Silencing of the human microsomal glucose-6-phosphate translocase induces glioma cell death: potential new anticancer target for curcumin. FEBS Lett;580:3746–3752.
7. Belkaid A., Fortier S., Cao J., Annabi B. (2007) Necrosis induction in glioblastoma cells reveals a new ``bioswitch'' function for the MT1-MMP/G6PT signaling axis in proMMP-2 activation versus cell death decision. Neoplasia;9:332–340.
8. Lord-Dufour S., Copland I.B., Levros L.C. Jr, Post M., Das A., Khosla C., Galipeau J., Rassart E., Annabi B. (2009) Evidence for transcriptional regulation of the glucose-6-phosphate transporter by HIF-1alpha: targeting G6PT with mumbaistatin analogs in hypoxic mesenchymal stromal cells. Stem Cells;27:489–497.
9. van Schaftingen E., Gerin I. (2002) The glucose-6-phosphatase system. Biochem J;362:513–532.
10. Chou J.Y., Matern D., Mansfield B.C., Chen Y.T. (2002) Type I glycogen storage diseases: disorders of the glucose-6-phosphatase complex. Curr Mol Med;2:121–143.
11. Kim S.Y., Nguyen A.D., Gao J.L., Murphy P.M., Mansfield B.C., Chou J.Y. (2006) Bone marrow-derived cells require a functional glucose 6-phosphate transporter for normal myeloid functions. J Biol Chem;281:28794–28801.
12. Yiu W.H., Pan C.J., Allamarvdasht M., Kim S.Y., Chou J.Y. (2007) Glucose-6-phosphate transporter gene therapy corrects metabolic and myeloid abnormalities in glycogen storage disease type Ib mice. Gene Ther;14:219–226.
13. Chen L.Y., Shieh J.J., Lin B., Pan C.J., Gao J.L., Murphy P.M., Roe T.F., Moses S., Ward J.M., Lee E.J., Westphal H., Mansfield B.C., Chou J.Y. (2003) Impaired glucose homeostasis, neutrophil trafficking and function in mice lacking the glucose-6-phosphate transporter. Hum Mol Genet;12:2547–2558.
14. Leuzzi R., Bánhegyi G., Kardon T., Marcolongo P., Capecchi P.L., Burger H.J., Benedetti A., Fulceri R. (2003) Inhibition of microsomal glucose-6-phosphate transport in human neutrophils results in apoptosis: a potential explanation for neutrophil dysfunction in glycogen storage disease type 1b. Blood;101:2381–2387.
15. Cheung Y.Y., Kim S.Y., Yiu W.H., Pan C.J., Jun H.S., Ruef R.A., Lee E.J., Westphal H., Mansfield B.C., Chou J.Y. (2007) Impaired neutrophil activity and increased susceptibility to bacterial

infection in mice lacking glucose-6-phosphatase-beta. J Clin Invest;117:784–793.
16. Fortier S., Labelle D., Sina A., Moreau R., Annabi B. (2008) Silencing of the MT1-MMP/G6PT axis suppresses calcium mobilization by sphingosine-1-phosphate in glioblastoma cells. FEBS Lett;582:799–804.
17. van de Werve G., Lange A., Newgard C., Méchin M.C., Li Y., Berteloot A. (2000) New lessons in the regulation of glucose metabolism taught by the glucose 6-phosphatase system. Eur J Biochem;267:1533–1549.
18. Ramakrishna N.V.S., Swamy K.H.S., Kumar E.K.S.V., Kushwaha M.M.S., Kota S., Raman D., Kurz M., Kogler H.. (1997) PCT/EP99/04127; WO 99-67408 A1; US 6,297,043 B1.
19. Lee T.S., Das A., Khosla C. (2007) Structure-activity relationships of semisynthetic mumbaistatin analogs. Bioorg Med Chem;15:5207–5218.
20. Hemmerle H., Burger H.J., Below P., Schubert G., Rippel R., Schindler P.W., Paulus E., Herling A.W. (1997) Chlorogenic acid and synthetic chlorogenic acid derivatives: novel inhibitors of hepatic glucose-6-phosphate translocase. J Med Chem;40:137–145.
21. Granado-Serrano A.B., Martín M.A., Izquierdo-Pulido M., Goya L., Bravo L., Ramos S. (2007) Molecular mechanisms of (-)-epicatechin and chlorogenic acid on the regulation of the apoptotic and survival/proliferation pathways in a human hepatoma cell line. J Agric Food Chem;55:2020–2027.
22. Belkaid A., Currie J.C., Desgagnés J., Annabi B. (2006) The chemopreventive properties of chlorogenic acid reveal a potential new role for the microsomal glucose-6-phosphate translocase in brain tumor progression. Cancer Cell Int;6:7.
23. Annabi B., Rojas-Sutterlin S., Laroche M., Lachambre M.P., Moumdjian R., Béliveau R. (2008) The diet-derived sulforaphane inhibits matrix metalloproteinase-9-activated human brain microvascular endothelial cell migration and tubulogenesis. Mol Nutr Food Res;52:692–700.
24. Roomi M.W., Monterrey J.C., Kalinovsky T., Rath M., Niedzwiecki A. (2009) Distinct patterns of matrix metalloproteinase-2 and -9 expression in normal human cell lines. Oncol Rep;21:821–826.
25. Lakka S.S., Gondi C.S., Rao J.S. (2005) Proteases and glioma angiogenesis. Brain Pathol;15:327–341.
26. Stins M.F., Gilles F., Kim K.S. (1997) Selective expression of adhesion molecules on human brain microvascular endothelial cells. J Neuroimmunol;76:81–90.
27. Greiffenberg L., Goebel W., Kim K.S., Weiglein I., Bubert A., Engelbrecht F., Stins M., Kuhn M. (1998) Interaction of Listeria monocytogenes with human brain microvascular endothelial cells: InlB-dependent invasion, long-term intracellular growth, and spread from macrophages to endothelial cells. Infect Immun;66:5260–5267.
28. McLaughlin N., Annabi B., Sik Kim K., Bahary J.P., Moumdjian R., Béliveau R. (2006) The response to brain tumor-derived growth factors is altered in radioresistant human brain endothelial cells. Cancer Biol Ther;5:1539–1545.
29. Lamy S., Gingras D., Béliveau R. (2002) Green tea catechins inhibit vascular endothelial growth factor receptor phosphorylation. Cancer Res;62:381–385.
30. Sina A., Lord-Dufour S., Annabi B. (2009) Cell-based evidence for aminopeptidase N/CD13 inhibitor actinonin targeting of MT1-MMP-mediated proMMP-2 activation. Cancer Lett;279:171–176.
31. Fortier S., Touaibia M., Lord-Dufour S., Galipeau J., Roy R., Annabi B. (2008) Tetra- and hexavalent mannosides inhibit the pro-apoptotic, antiproliferative and cell surface clustering effects of concanavalin-A: impact on MT1-MMP functions in marrow-derived mesenchymal stromal cells. Glycobiology;18:195–204.
32. Auerbach R., Lewis R., Shinners B., Kubai L., Akhtar N. (2003) Angiogenesis assays: a critical overview. Clin Chem;49:32–40.
33. Abécassis I., Olofsson B., Schmid M., Zalcman G., Karniguian A. (2003) RhoA induces MMP-9 expression at CD44 lamellipodial focal complexes and promotes HMEC-1 cell invasion. Exp Cell Res;291:363–376.
34. Handsley M.M., Edwards D.R. (2005) Metalloproteinases and their inhibitors in tumor angiogenesis. Int J Cancer;115:849–860.
35. Noël A., Jost M., Maquoi E. (2008) Matrix metalloproteinases at cancer tumor-host interface. Semin Cell Dev Biol;19:52–60.
36. Karin M. (2008) The IkappaB kinase - a bridge between inflammation and cancer. Cell Res;18:334–342.
37. Massaro M., Zampolli A., Scoditti E., Carluccio M.A., Storelli C., Distante A., De Caterina R. (2010) Statins inhibit cyclooxygenase-2 and matrix metalloproteinase-9 in human endothelial cells: anti-angiogenic actions possibly contributing to plaque stability. Cardiovasc Res (in press).
38. Agius L., Centelles J., Cascante M. (2002) Multiple glucose 6-phosphate pools or channelling of flux in diverse pathways? Biochem Soc Trans;30:38–43.
39. Sweet I.R., Gilbert M., Maloney E., Hockenbery D.M., Schwartz M.W., Kim F. (2009) Endothelial inflammation induced by excess glucose is associated with cytosolic glucose 6-phosphate but not increased mitochondrial respiration. Diabetologia;52:921–931.
40. Ghosh A., Cheung Y.Y., Mansfield B.C., Chou J.Y. (2005) Brain contains a functional glucose-6-phosphatase complex capable of endogenous glucose production. J Biol Chem;280:11114–11119.
41. Strauss L.G., Koczan D., Klippel S., Pan L., Cheng C., Willis S., Haberkorn U., Dimitrakopoulou-Strauss A. (2008) Impact of angiogenesis-related gene expression on the tracer kinetics of 18F-FDG in colorectal tumors. J Nucl Med;49:1238–1244.
42. Lidgren A., Bergh A., Grankvist K., Rasmuson T., Ljungberg B. (2008) Glucose transporter-1 expression in renal cell carcinoma and its correlation with hypoxia inducible factor-1α. BJU Int;101:480–484.
43. Burgman P., O'Donoghue J.A., Humm J.L., Ling C.C. (2001) Hypoxia-induced increase in FDG uptake in MCF7 cells. J Nucl Med;42:170–175.
44. Maxwell P.H., Dachs G.U., Gleadle J.M., Nicholls L.G., Harris A.L., Stratford I.J., Hankinson O., Pugh C.W., Ratcliffe P.J. (1997) Hypoxia-inducible factor-1 modulates gene expression in solid tumors and influences both angiogenesis and tumor growth. Proc Natl Acad Sci USA;94:8104–8109.
45. Marín-Hernández A., Gallardo-Pérez J.C., Ralph S.J., Rodríguez-Enríquez S., Moreno-Sánchez R. (2009) HIF-1alpha modulates energy metabolism in cancer cells by inducing over-expression of specific glycolytic isoforms. Mini Rev Med Chem;9:1084–1101.
46. Annabi B., Naud E., Lee Y.T., Eliopoulos N., Galipeau J. (2004) Vascular progenitors derived from murine bone marrow stromal

cells are regulated by fibroblast growth factor and are avidly recruited by vascularizing tumors. J Cell Biochem;91:1146–1158.
47. Birnbaum T., Roider J., Schankin C.J., Padovan C.S., Schichor C., Goldbrunner R., Straube A. (2007) Malignant gliomas actively recruit bone marrow stromal cells by secreting angiogenic cytokines. J Neurooncol;83:241–247.
48. Yuan H., Gaber M.W., Boyd K., Wilson C.M., Kiani M.F., Merchant T.E. (2006) Effects of fractionated radiation on the brain vasculature in a murine model: blood–brain barrier permeability, astrocyte proliferation, and ultrastructural changes. Int J Radiat Oncol Biol Phys;66:860–866.
49. Jadhav U., Chigurupati S., Lakka S.S., Mohanam S. (2004) Inhibition of matrix metalloproteinase-9 reduces in vitro invasion and angiogenesis in human microvascular endothelial cells. Int J Oncol;25:1407–1414.
50. Annabi B., Currie J.C., Moghrabi A., Béliveau R. (2007) Inhibition of HuR and MMP-9 expression in macrophage-differentiated HL-60 myeloid leukemia cells by green tea polyphenol EGCg. Leuk Res;31:1277–1284.
51. López de Silanes I., Fan J., Galbán C.J., Spencer R.G., Becker K.G., Gorospe M. (2004) Global analysis of HuR-regulated gene expression in colon cancer systems of reducing complexity. Gene Expr;12:49–59.
52. Levy A.P. (1998) Hypoxic regulation of VEGF mRNA stability by RNA-binding proteins. Trends Cardiovasc Med;8:246–250.
53. Sheflin L.G., Zou A.P., Spaulding S.W. (2004) Androgens regulate the binding of endogenous HuR to the AU-rich 3′UTRs of HIF-1alpha and EGF mRNA. Biochem Biophys Res Commun;322:644–651.
54. Demeule M., Régina A., Annabi B., Bertrand Y., Bojanowski M.W., Béliveau R. (2004) Brain endothelial cells as pharmacological targets in brain tumors. Mol Neurobiol;30:157–183.
55. McLaughlin N., Annabi B., Lachambre M.P., Kim K.S., Bahary J.P., Moumdjian R., Béliveau R. (2006) Combined low dose ionizing radiation and green tea-derived epigallocatechin-3-gallate treatment induces human brain endothelial cells death. J Neurooncol;80:111–121.
56. Bian C., Zhao K., Tong G.X., Zhu Y.L., Chen P. (2005) Immortalization of human umbilical vein endothelial cells with telomerase reverse transcriptase and simian virus 40 large T antigen. J Zhejiang Univ Sci B;6:631–636.